ACS Catalysis

pubs.acs.org/acscatalysis Research Article

Design and Synthesis of Chiral Bidentate Phosphine-Free 2-Hydroxypyridine-Oxazoline Ligands for Manganese-Catalyzed Hydrogenation

Gao-Wei Wang, Mu-Wang Chen,* Ya-Qi Wu, Qing-Xian Xie, Zheng Liu, Rong-Zhen Liao,* and Yong-Gui Zhou*

Cite This: *ACS Catal.* 2025, 15, 3418−3427 Read Online

ACCESS | Metrics & More | Article Recommendations | Supporting Information

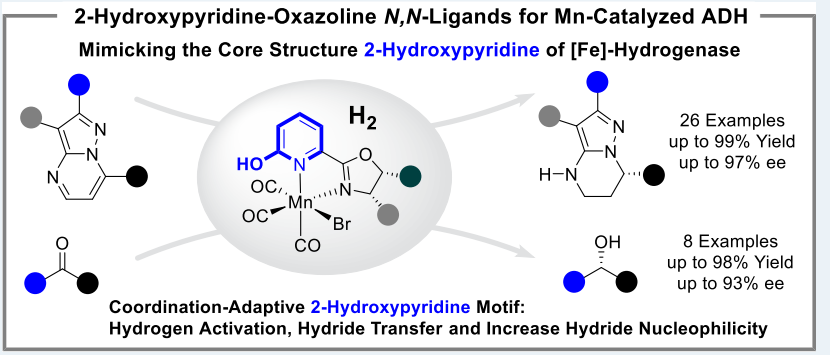

ABSTRACT: Significant progress has been made in the development of tridentate phosphine ligands for manganese-catalyzed asymmetric direct hydrogenation (ADH). However, their high cost and susceptibility to oxidation limit their further application. In contrast, bidentate phosphine-free ligands, such as bidentate nitrogen-based ligands, remain underexplored in the context of manganese-catalyzed asymmetric hydrogenation. Herein, we have developed a series of chiral 2-hydroxypyridine-oxazoline ligands with tunable steric and electronic properties. These ligands are characterized by exhibiting tautomerism between 2-hydroxypyridine and pyridone, which enhances hydrogen activation, hydride transfer, and nucleophilicity of the hydride species. They were applied in manganese-catalyzed asymmetric hydrogenation of heteroaromatics, simple ketones, and ketimines with high yields and enantioselectivities. Preliminary mechanistic studies and DFT calculations revealed the critical role of the ligand in facilitating manganese-catalyzed asymmetric hydrogenation, shedding light on the possible catalytic pathways. These findings demonstrate the promising potential of chiral 2-hydroxypyridine-oxazoline ligands as an efficient *N*,*N*-ligand scaffold for asymmetric catalysis.

KEYWORDS: *2-hydroxypyridine-oxazoline ligands, phosphine-free, manganese, asymmetric hydrogenation*

INTRODUCTION

Manganese has emerged as a promising alternative to conventional transition metal catalysts in hydrogenation and dehydrogenation processes, owing to its abundance, low toxicity, and cost-effectiveness.[1] In 2016, the Beller group pioneered manganese-catalyzed hydrogenation reactions.[2] Building on this progress, manganese-catalyzed asymmetric direct hydrogenation (ADH) of C═O, C═N, and heteroaromatics using NNP and PNP ligands has been explored by researchers such as Clarke, Beller, Ding, Zhang, Zhong, and Liu (Scheme 1a).[3,4] The development of these tridentate phosphine-containing ligands has significantly advanced the application of manganese-catalyzed hydrogenation reactions. Despite these achievements, the field still requires the development of new chiral ligands for manganese catalysis. Tridentate phosphine ligands, though effective, are costly and prone to oxidation, complicating them difficult to synthesize.[5]

In contrast, bidentate phosphine-free ligands, such as nitrogen-based ligands, remain relatively underexplored in manganese-catalyzed asymmetric direct hydrogenation.[1d] Notably, Sortais and Sun groups have successfully employed phosphine-free bidentate ligands in manganese-catalyzed asymmetric transfer hydrogenation (ATH), underscoring the potential for further development.[5,6] Thus, the engineering of novel chiral phosphine-free ligands could be pivotal in enhancing the efficiency of manganese-catalyzed asymmetric hydrogenation reactions.

Received: October 19, 2024
Revised: January 12, 2025
Accepted: January 15, 2025
Published: February 11, 2025

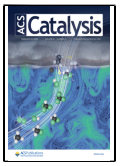

Scheme 1. Design, Synthesis (a–c), and Application (d) of Chiral 2-Hydroxypyridine Ligands for Mn-Catalyzed ADH

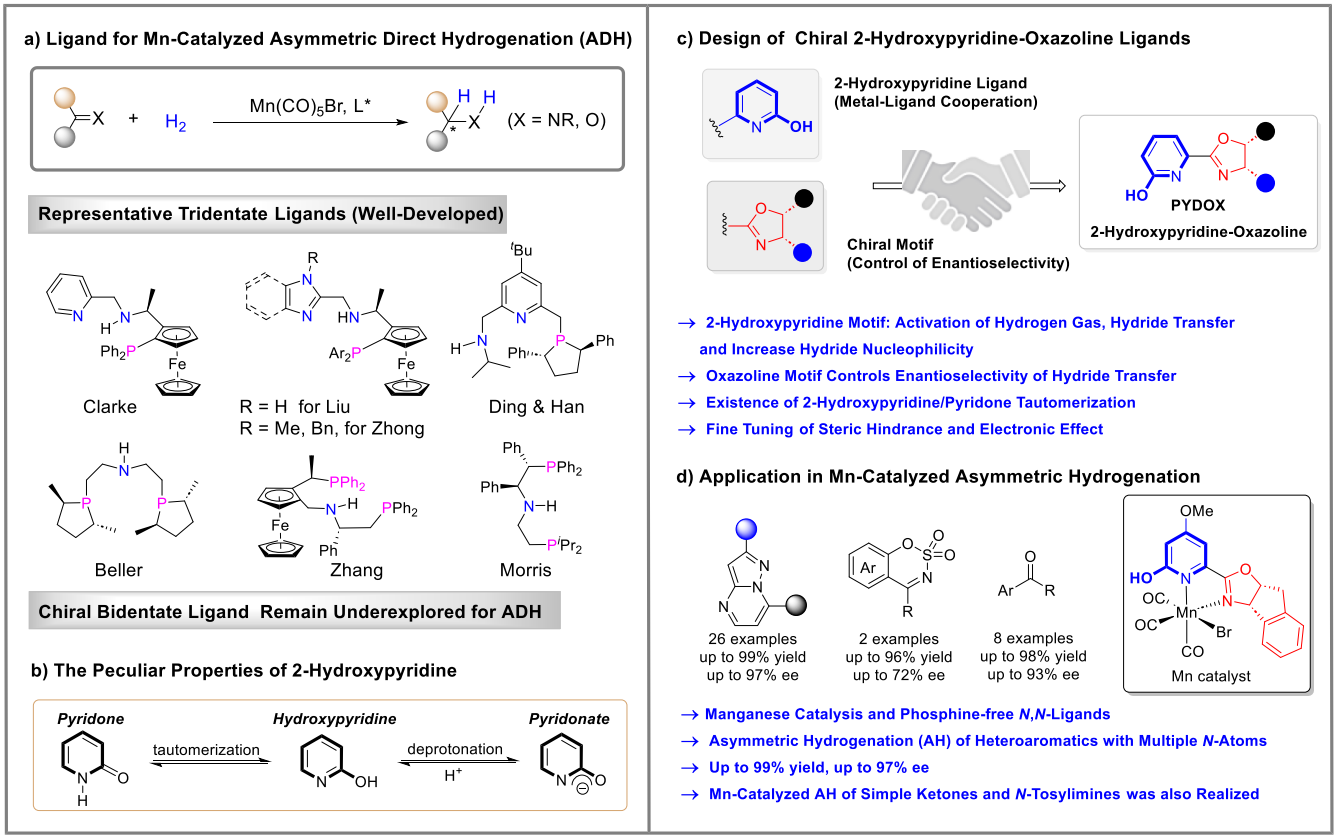

Scheme 2. Synthesis of the Chiral 2-Hydroxypyridine-oxazoline Ligands

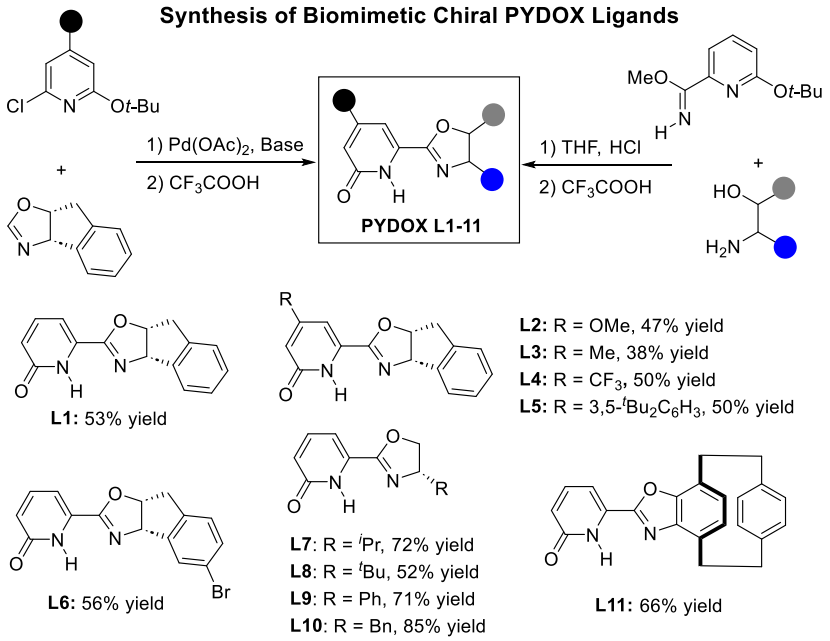

The 2-hydroxypyridine framework is the core structure of [Fe]-hydrogenases,[7] consisting of three forms: pyridone, hydroxypyridine, and pyridonate (Scheme 1b).[8] The interaction between these species and the metal center is critical for hydrogen activation and hydrogen transfer.[8b] Researchers have been inspired by the unique properties of 2-hydroxypyridine to design new catalysts and ligands. To date, a series of ligands containing the 2-hydroxypyridine structural unit have been designed and applied to transition metal-catalyzed reactions.[9−13] Despite great progress in synthesis and application of 2-hydroxypyridine-based ligands, the development of chiral versions has lagged behind due to the inherent lack of a chiral environment in the 2-hydroxypyridine motif. Consequently,

https://doi.org/10.1021/acscatal.4c06422
ACS Catal. 2025, 15, 3418−3427

there are few reports on the application of 2-hydroxypyridine ligands in asymmetric reactions.[14]

The oxazoline-containing ligands are an important class of chiral ligands widely used in various metal-catalyzed asymmetric catalysis.[15] Considering that the 2-hydroxypyridine unit plays a crucial role in hydrogen activation and hydride transfer, we envisioned synthesizing the bidentate 2-hydroxypyridine-oxazoline *N,N*-ligands by a combination of the achiral 2-hydroxypyridine and chiral oxazoline skeletons. These novel chiral ligands are expected to take advantage of the benefits of oxazoline along with the unique functionalities of 2-hydroxypyridine. The chiral 2-hydroxypyridine-oxazoline ligands offer several features and advantages: (1) the reciprocal isomerism of 2-hydroxypyridine and pyridone allows fine-tuning of the catalytic reaction at the primitive reaction step,[16] (2) the presence of pyridone or 2-hydroxypyridine forms in the complex provides dual metal−ligand cooperation functions, enhancing the reactivity and enantioselectivity of the hydrogenation, and (3) the ligand's steric hindrance and electronic effects are easily adjusted, facilitating precise control over the catalytic process (Scheme 1c). Herein, we reported the rational design and synthesis of novel chiral 2-hydroxypyridine-oxazoline ligands (PYDOX),[17] and their application in manganese-catalyzed asymmetric hydrogenation of the heteroaromatics, simple ketones, and *N*-sulfonylimines with high yields and excellent enantioselectivities (Scheme 1d).

RESULTS AND DISCUSSION

The chiral pyridin-2(1*H*)-one/oxazoline *N,N*-ligands (abbreviated as **PYDOX**) could be synthesized through two methods according to similar procedures (Scheme 2).[18−20] One is palladium-catalyzed coupling of 2-(*tert*-butoxy)-6-chloro-pyridine and the chiral dihydrooxazole,[18] followed by the deprotection with trifluoroacetic acid.[19] The other is annulation of imidoester with chiral amino alcohols,[20] followed by deprotection with trifluoroacetic acid. Notably, the structures of all ligands are in the form of pyridone (see the Supporting Information for details).

With PYDOX ligands in hand, we began exploring their application in the asymmetric hydrogenation of pyrazolo[1,5-*a*]pyrimidines. Chiral 4,5,6,7-tetrahydropyrazolo[1,5-*a*]-pyrimidine is a valuable and common substructure found in bioactive molecules and pharmaceuticals.[21] Therefore, the preparation has attracted great attention[22] and one of most straightforward and atom-economic ways is the direct asymmetric hydrogenation of the pyrazolo[1,5-*a*]pyrimidines. However, this method is still in its infancy due to the strong aromatic stability leading to lower reactivity as well as the substrate contains multiple nitrogen atoms that may coordinate with the catalyst to inhibit the reactivity of the chiral catalyst.[23] Until recently, the synthesis of chiral 4,5,6,7-tetrahydropyrazolo[1,5-*a*]pyrimidines via noble metal-catalyzed asymmetric hydrogenation was developed.[24] Therefore, the development of new earth-abundant metal-catalyzed asymmetric hydrogenation of pyrazolo[1,5-*a*]pyrimidines is still necessary.

Initially, we chose 2,7-diphenylpyrazolo[1,5-*a*]pyrimidine **1a** as a model substrate, $Mn(CO)_5Br$ as a metal precursor, PYDOX **L1** as the ligand, and KO^{i}Pr as the base for the reaction in DCE at 80 °C under hydrogen gas (750 psi). To our delight, the desired hydrogenation product **2a** was obtained in 98% yield with 93% enantioselectivity (93% ee). The solvents played a crucial role in both reactivity and enantioselectivity, as shown in Table 1 (entries 1−5). The hydrogenation proceeded smoothly in DCM, 1,4-dioxane, and

Table 1. Condition Optimization[a]

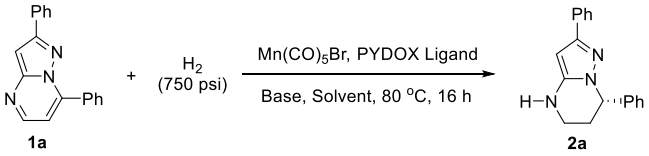

entry	solvent	base	ligand	yield (%)[b]	e.e.[c]
1	DCE	KO^{i}Pr	**L1**	98	93
2	DCM	KO^{i}Pr	**L1**	95	89
3	1,4-dioxane	KO^{i}Pr	**L1**	78	84
4	THF	KO^{i}Pr	**L1**	86	74
5	toluene	KO^{i}Pr	**L1**	98	83
6	DCE	KO^{t}Bu	**L1**	98	93
7	DCE	NaO^{t}Bu	**L1**	n.r	
8	DCE	LiO^{t}Bu	**L1**	n.r	
9	DCE	Cs_2CO_3	**L1**	98	82
10	DCE	K_3PO_4	**L1**	97	93
11	DCE		**L1**	n.r	
12[d]	DCE	KO^{i}Pr	**L1**	80	93
13[e]	DCE	KO^{i}Pr	**L1**	96	93
14	DCE	KO^{i}Pr	**L2**	96	96
15	DCE	KO^{i}Pr	**L3**	95	95
16	DCE	KO^{i}Pr	**L4**	38	91
17	DCE	KO^{i}Pr	**L5**	27	75
18	DCE	KO^{i}Pr	**L6**	84	84
19	DCE	KO^{i}Pr	**L7**	75	66
20	DCE	KO^{i}Pr	**L8**	98	87
21	DCE	KO^{i}Pr	**L9**	88	53
22	DCE	KO^{i}Pr	**L10**	82	49
23	DCE	KO^{i}Pr	**L11**	15	63
24[f]	DCE	KO^{i}Pr	**L2**	97	97
25[g]	**DCE**	**KO^{i}Pr**	**L2**	**98**	**97**

[a]Reaction conditions: **1a** (0.20 mmol), $Mn(CO)_5Br$ (2.0 mol %), **L** (2.2 mol %), base (7.5 mol %), solvent (2.0 mL), 80 °C, and 16 h. [b]Yield was measured by analysis of ^{1}H NMR spectra, using 1,3,5-trimethoxybenzene as the internal standard. [c]Determined by chiral HPLC. [d]Base (2.5 mol %). [e]Base (5.0 mol %). [f]70 °C. [g]H_2 (600 psi).

THF with excellent reactivity and good enantioselectivity. Next, a series of bases were screened (entries 6−10), and the best results were achieved using KO^{i}Pr. In the absence of a base, the reaction did not proceed (entry 11). The yield and enantioselectivity were maintained even when the base loading was reduced to 5 mol % (entry 13). Encouraged by these results, the steric and electronic effects of the ligands were investigated (entries 14−23). The electron-rich ligand PYDOX **L2** had a favorable impact, giving excellent results (96% yield and 96% ee). Furthermore, the effects of the temperature and hydrogen pressure on the reactivity and enantioselectivity were also examined (entries 24−25). Optimal results were obtained at a reaction temperature of 70 °C and a hydrogen pressure of 600 psi, affording the product with 98% yield and 97% ee (see the Supporting Information for more details).

With the optimized conditions in hand, the substrate scope was investigated. To ensure complete consumption of all substrates, we conducted the substrate scope expansion with a catalyst loading of 4 mol %. A wide variety of pyrazolo[1,5-*a*]pyrimidines were examined, as shown in Scheme 3. First, the electronic properties and positions of the substituents on the

https://doi.org/10.1021/acscatal.4c06422
ACS Catal. 2025, 15, 3418−3427

Scheme 3. Substrate Scope of Pyrazolo[1,5-*a*]Pyrimidines

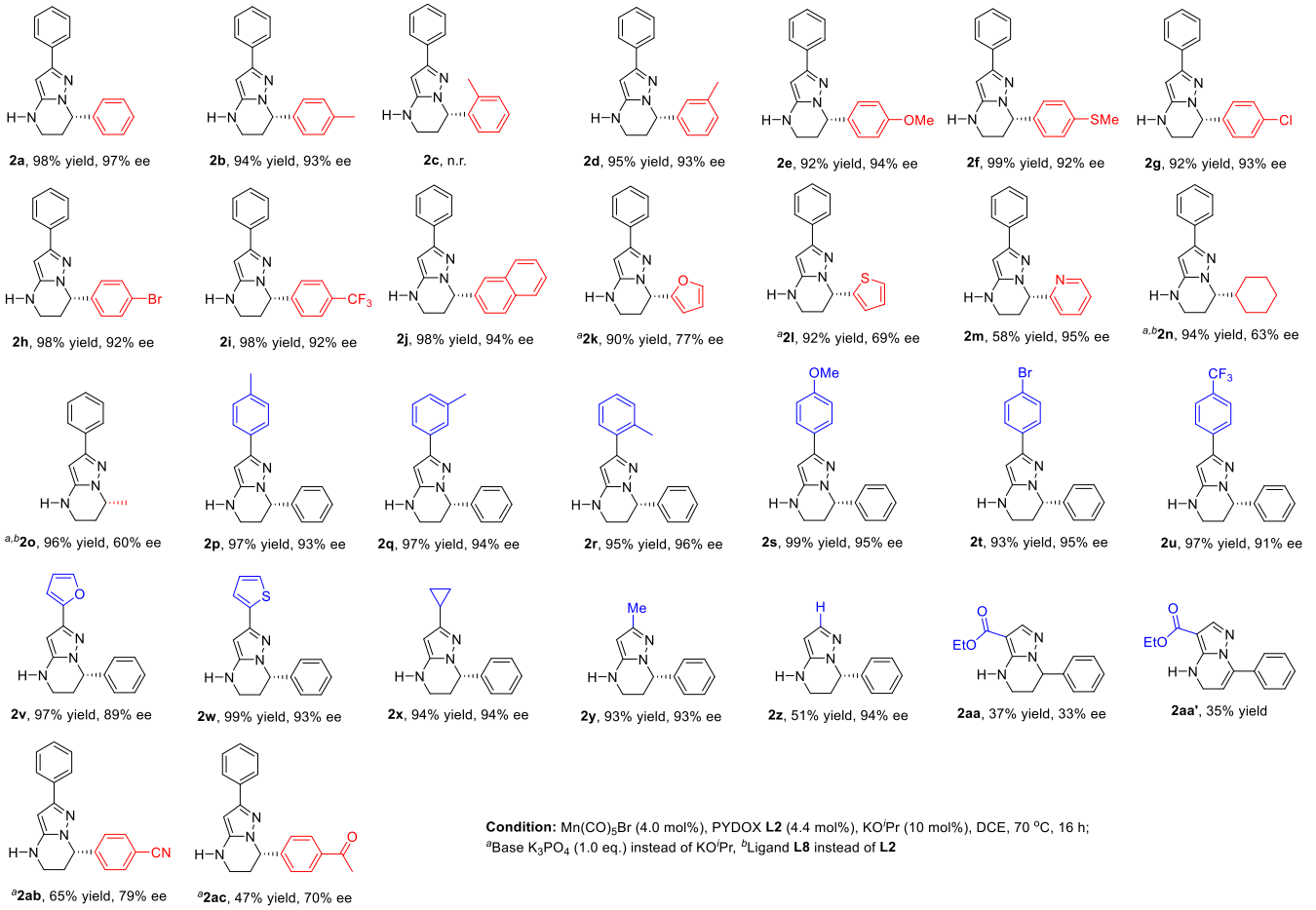

phenyl of C7 were evaluated. Substitution at the *para* or *meta* positions with a methyl group resulted in excellent yields and enantioselectivities (**2b** and **2d**). Unfortunately, no product was obtained with substitution at the *ortho*-position due to significant steric hindrance (**2c**). Various electron-donating or electron-withdrawing substituents at the *para*-position of phenyl at C7 were tolerated, giving the products with 92−99% yields with 92−94% ees (**2e**−**2i**). Notably, a 2-naphthyl-substituent (**2j**) performed well, providing an excellent yield and enantioselectivity. However, the catalyst showed low reactivity and enantioselectivity for heteroaromatic substituents (**2k**−**2l**) under the standard conditions. To our delight, excellent yields and moderate enantioselectivities were obtained with K_3PO_4 instead of KO^{i}Pr. Meanwhile, this methodology was also compatible with a pyridine substituent (**2m**), despite its strong catalyst toxicity, giving a chiral product with a moderate yield (58%) and excellent enantioselectivity (95% ee). For alkyl substituents at the C7 position, such as cyclohexyl (**2n**) and methyl (**2o**), poor reactivity and enantioselectivity were observed under the standard conditions, likely due to the absence of $\pi-\pi$ interactions between the substrate and the catalyst. Gratifyingly, excellent yields and moderate enantioselectivities were obtained by replacing KO^{i}Pr with K_3PO_4 and using sterically hindered chiral ligand **L8**.

Furthermore, a series of substituents at the C2 position were also investigated (**2p**−**2y**). The electronic properties and positions of the phenyl group had a marginal effect on the enantioselectivity and activity. Most substrates yielded the corresponding products in excellent yields (93−99%) and enantioselectivities (89−96% ee). Additionally, heteroaromatic and alkyl substituents at C2 were compatible, giving the desirable products with excellent yields and ee values (**2v**−**2y**). Even when the substituent at the C2 position was a hydrogen atom, a moderate yield (51%) and excellent enantioselectivity (94% ee) were achieved (**2z**). Interestingly, the substrate **1aa** with an ester group at the 3-position gave the desired product **2aa** under the standard conditions and generated a partially hydrogenated product **2aa′**. However, due to its low ee value, its absolute configuration has not been determined. This observation could aid further mechanistic studies. Finally, substrates **1ab** and **1ac** containing functional groups that are reductant-sensitive were also evaluated. However, both substrates yielded only moderate product yields and enantioselectivities.

To further extend the generality of the PYDOX ligands in manganese-catalyzed asymmetric hydrogenation, we investigated the scope of asymmetric hydrogenation for simple ketones and cyclic *N*-sulfonylimines with slight adjustments to the standard conditions. For simple ketone substrates (**4a**−**4h**), the desired alcohol products were obtained in moderate to excellent yields (40−98%) and good enantioselectivities (79−93% ee). In addition, for cyclic *N*-sulfonylimine substrates (**4i** and **4j**), excellent yields (93% and 96%) and moderate enantioselectivities (69% and 72% ee) were also observed (Scheme 4).

https://doi.org/10.1021/acscatal.4c06422
ACS Catal. 2025, 15, 3418−3427

Scheme 4. Substrate Scope: Ketones and *N*-Sulfonylimines

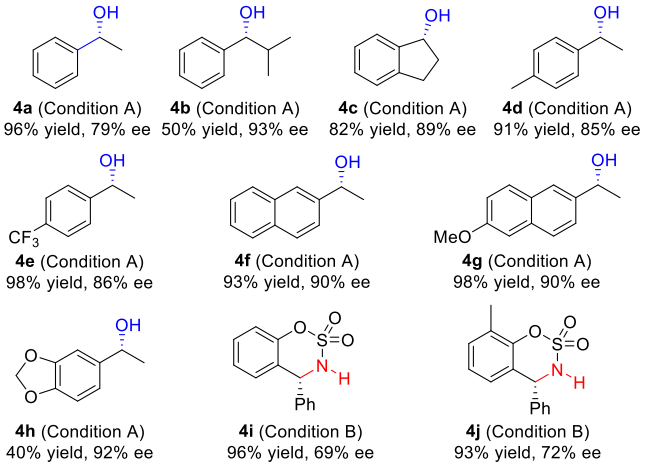

Condition A: H_2 (700 psi), $Mn(CO)_5Br$ (2.5 mol%), **L11** (5.0 mol%), $K_3PO_4 \cdot 3H_2O$ (10 mol%), toluene, 80 °C, 24 h

Condition B: H_2 (750 psi), $Mn(CO)_5Br$ (2.0 mol%), Ligand **L8** (2.2 mol%), KO^iPr (5.0 mol%), THF, 50 °C, 24 h

To demonstrate the efficiency of this catalytic system, a gram-scale experiment on asymmetric hydrogenation of heteroaromatics **1a** was conducted under the standard condition, affording the desirable product with excellent yield (95%) and enantiomeric excess (93% ee) without significant loss of reactivity and enantioselectivity (Scheme 5).

Scheme 5. Experiment at Gram Scale

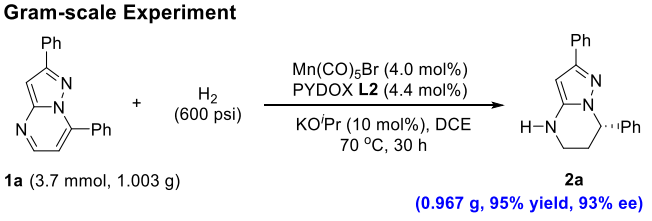

To explore the structural forms (pyridone, hydroxypyridine, and pyridonate) and function of the 2-hydroxypyridine ligand during the hydrogenation, as well as the detailed mechanism, a series of experiments were performed including control experiments, X-ray diffraction analysis of manganese complex, deuterium labeling experiment, and intermediate capture experiments.

To verify the importance of the hydroxyl groups in PYDOX ligands, commonly used pyridine-oxazoline ligand **In-Pyox** and hydroxyl-protected ligand **In-^{5}MeOPyox** were tested as substitutes for the PYDOX ligand. Both failed to yield the desired product, indicating that the hydroxyl group in the PYDOX ligand plays a crucial role (Scheme 6a).

Structural Forms of 2-Hydroxypyridine during the Reaction. Initially, ^{1}H NMR analysis showed that the PYDOX ligands were in the pyridone form, but they converted to the 2-hydroxypyridine form upon complexation with $Mn(CO)_5Br$.[25] This conversion was verified by synthesizing the $Mn(CO)_5Br$-**L6** complex, and its structure was determined via X-ray diffraction analysis (Scheme 6b).[26] Subsequently, the complex of $Mn(CO)_5Br$ and **L1** was reacted with $K_3PO_4 \cdot 3H_2O$ in THF, yielding a new complex (Scheme 6c). This new complex was characterized by HRMS, confirming the pyridone form (see the Supporting Information for details). Additionally, the hydrogenation process requires the presence of a base, indicating that the ligand could be mutually converted between the pyridone and pyridonate under basic condition. During hydrogenation, the pyridonate form activates hydrogen and enhances catalytic activity by the interaction of the O−H or the O−M groups with the substrate.

To further elucidate the reaction pathway, potential manganese intermediates in the hydrogenation reaction were investigated. In widely used Noyori-type hydrogenation catalysts, the "N−H" moiety stabilizes the transition state of the rate-determining step through hydrogen bonding with the substrate.[27] In 2014, Gordon's group first reported the formation of "N−M" moieties under basic conditions,[27b] and recently, Liu's group also proposed the "N−M" moiety (M = alkali metals) and characterized its structure. Kinetic studies indicated that the rate of hydride transfer from HMn−NM to ketone is 24 times faster than from HMn−NH, suggesting that the "N−M" effect may be more suitable for hydrogenation reaction than the "N−H" effect.[28a] In manganese complexes containing a 2-hydroxypyridine unit, a similar phenomenon may occur,[25] where the "O−M" effect is more suitable than the "O−H" effect. To capture the HMn-OM species, we conducted NMR experiments. The $Mn(CO)_5Br$ and **L1** complex was prepared in situ, treated with KO^iPr, and then exposed to hydrogen gas in an NMR tube at 70 °C for 1 h. The NMR tube was then cooled to room temperature, and the ^{1}H NMR spectra were quickly collected (Scheme 6d). According to the literature,[6b,28] "Mn−H" may have a noncovalent interaction with K^+, resulting in a high-field chemical shift (−7.83 ppm). This also confirms the existence of pyridonate forms (see the Supporting Information for details). These results indicated that the chiral 2-hydroxypyridine-oxazoline ligand exists in three structural forms: pyridone, hydroxypyridine, and pyridonate.

Experimental Evidence of the "O−K" Effect. To demonstrate the "O−K" effect, organic bases such as DBU or Et_3N were used to replace KO^iPr under the standard conditions, but no reaction occurred (Scheme 6e). In addition, adding 18-crown-6 to chelate K^+ under the same conditions also resulted in no reaction. These experimental results suggest that the "O−K" effect is essential for the manganese-catalyzed hydrogenation reaction.

Deuterium Labeling Experiment. To verify the pathway of the hydrogenation of pyrazolo[1,5-*a*]pyrimidines, a deuterium labeling experiment was conducted by substituting deuterium for hydrogen gas in the asymmetric hydrogenation of **1a** (Scheme 6f). To avoid H-D exchange between the active hydrogen of 2-propanol in the KO^iPr solution and the substrate, K_3PO_4 was used as the base. After 24 h, deuterium incorporation at the 5- and 7-positions of the obtained product was greater than 99%, while at the 6-position, it was 30% and 60%, respectively. These results suggest that the hydrogenation reaction may proceed via initial 4,7-hydrogenation (deuterium incorporation at the 7-position >99%), followed by fast imine/enamine tautomerization (deuterium incorporation at the 6-position 30% and 60%), and final hydrogenation of the imine (deuterium incorporation at the 5-position >99%).

DFT Calculations. Density functional calculations[29] were performed to elucidate the mechanism and selectivity of this catalytic hydrogenation reaction. With KO^iPr as the base, which prefers to be in a tetrameric form in an aprotic solvent,[30] the deprotonation and bromide dissociation from the

https://doi.org/10.1021/acscatal.4c06422
ACS Catal. 2025, 15, 3418−3427

Scheme 6. Mechanistic Study Experiments

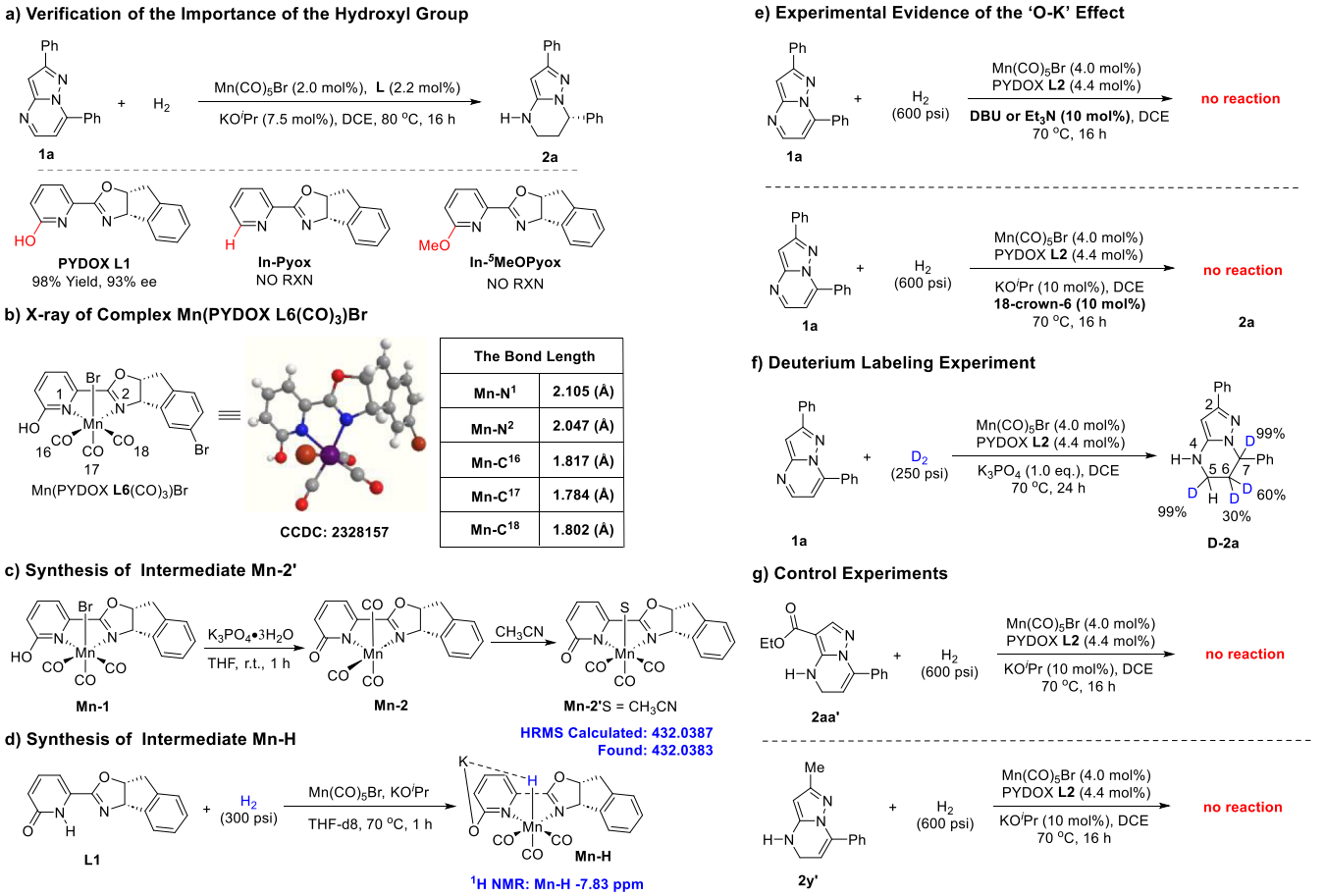

PYDOXMn(CO)$_3$Br complex was calculated to be exergonic by more than 30 kcal/mol (Scheme S2 in the Supporting Information). This leads to the formation of the catalytic resting state species **Int0** (Figure 1), in which three K^+ ions interact with the pyridone oxygen atom, and one O^{i}Pr anion is ligated to the Mn^I center. H_2 can react with **Int0** via a heterolytic H−H bond cleavage (**TS1**), in which the hydride is coordinated to the Mn^I center and the proton is delivered to the O^{i}Pr anion. This step is associated with a barrier of 25.9 kcal/mol, which turns out to be the rate-limiting step for the entire hydrogenation reaction. The generation of the Mn^I-hydride intermediate **Int1** is close to isogonic.

With **1a** as the model substrate, the hydrogenation reaction starts with the ligand exchange of the isopropanol by the substrate, leading to the formation of **Int2**, in which the pyridine nitrogen is coordinated to one of the K^+ ions. The following hydride transfer could occur at either the Re or *Si* face of the substrate plane, leading to the generation of a chiral carbon center at the C4 position. The barriers of the two transition states **TS2**-*S* and **TS2**-*R* were calculated to be 12.6 and 14.4 kcal/mol relative to **Int2**, respectively. The barrier difference of 1.8 kcal/mol corresponds to a computed ee of 86.7%, which agrees well with the experimental value of 93% at 70 °C. In this pathway, the hydride is at the axial up position (away from the indanyl moiety Mode a). It should be noted that two other plausible hydride binding modes have been considered as well in which the hydride is at the axial down position (close to the indanyl moiety, Mode b) or the equatorial position (*trans* to the oxazoline ligand, Mode c). The Gibbs energy diagram for these two possibilities is displayed in Figure S2. The barriers for Modes b and c are higher than those of Mode a. In addition, the hydride transfer to the C2 position has been explored (Figure S3), and the barrier was calculated to be 9.2 kcal/mol higher than that of **TS2**-*S*.

In order to understand the origin of the stereoselectivity, the local chiral environment in **TS2**-*S* is analyzed by the steric counter map (Figure S4) proposed by the Cavallo group.[31] The map is divided into four parts, namely, northeast (NE), southeast (SE), southwest (SW), and northwest (NW). Due to the presence of the K_4(O^{i}Pr)$_3$ group and the coordination interaction between substrate pyridine nitrogen and K^+, the zone SW is better to accommodate the phenyl pyrazolo group as it has less buried volume percentage compared with zone NE, thus favoring the *S* product. The energy decomposition analysis on **TS2**-*S* and **TS2**-*R* was also conducted using sobEDA.[32] As shown in Figure S5, the exchange-repulsion between the substrate and catalyst, which is smaller in **TS2**-*S*, plays an important role in dictating the selectivity. The role of the K_4(O^{i}Pr)$_3$ group has also been analyzed by optimizing the transition states without the K_4(O^{i}Pr)$_3$ group (Figure S6). Interestingly, the barrier of transition state **TS 2d**-*R* now becomes 1.7 kcal/mol lower than **TS 2d**-*S*, further supporting the critical role of KO^{i}Pr in the selectivity.

To further validate the proposed reaction pathway, the stereoselectivity for the hydrogenation of acetophenone was investigated (Figure S7). Mode a is also preferred, and the barrier of **TS2**−**4a**-*R* is 1.5 kcal/mol lower than that of **TS2**−

https://doi.org/10.1021/acscatal.4c06422
ACS Catal. 2025, 15, 3418−3427

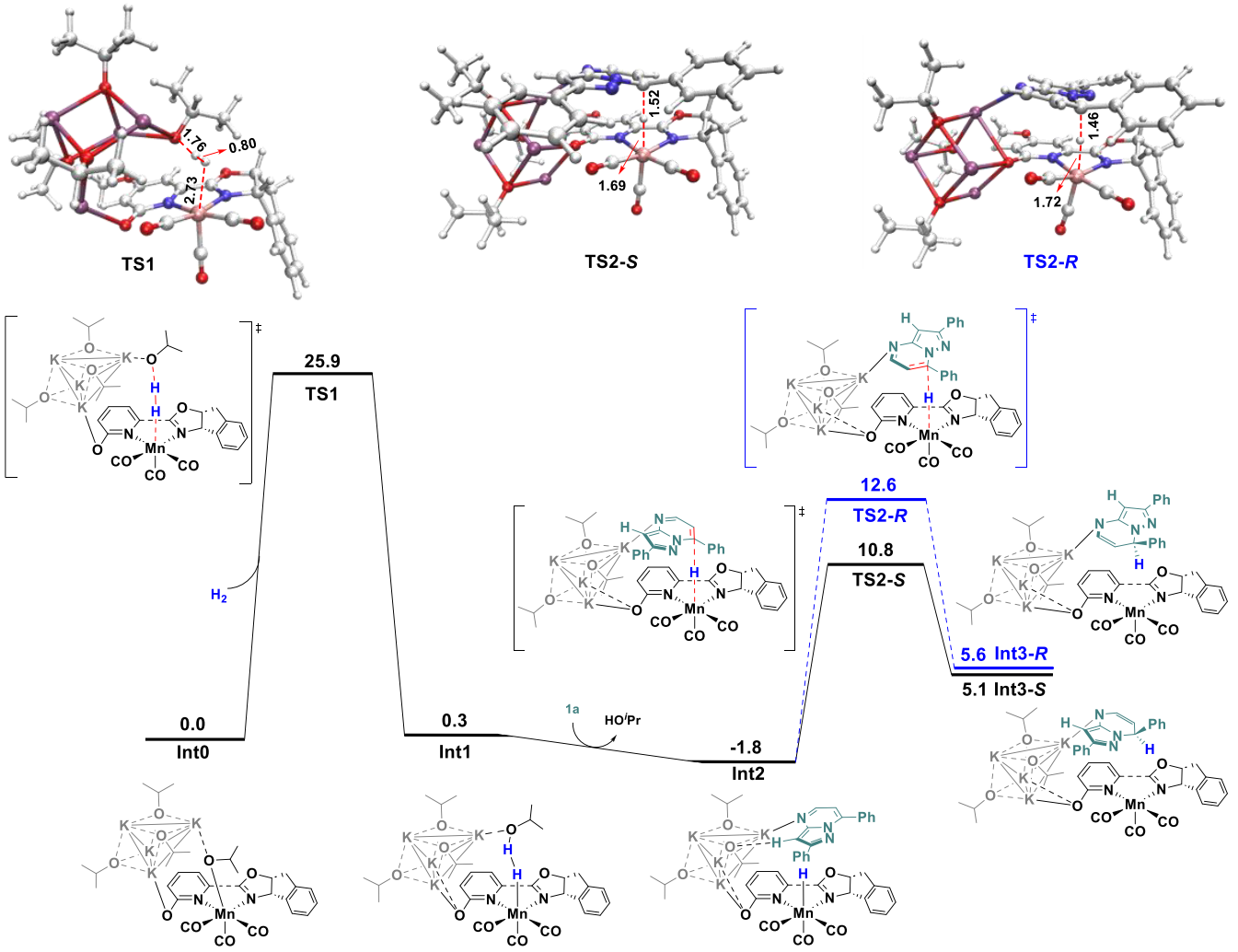

Figure 1. Gibbs energy profile (in kcal/mol) and structures of key transition states for the first hydrogenation of **1a** catalyzed by the Mn complex. Distances are given in Angstrom.

4a-*S*. This barrier difference can be converted to an ee of 78.9% at 80 °C (experimental value of 79%).

The mechanism of the second hydrogenation (Figure S8) is very similar to that of the first one. The hydride transfer is quite facile, and the hydrogenation is exergonic by 10.9 kcal/mol.

Control Experiments. To further understand the detailed process of manganese-catalyzed asymmetric hydrogenation of pyrazolo[1,5-*a*]pyrimidines, the 4,5-semihydrogenation intermediate **2aa′** and **2y′** were synthesized and subjected to the hydrogenation under the standard condition (Scheme 6g). The reaction did not proceed, indicating that 4,5-semihydrogenation intermediates may not be key intermediates in the hydrogenation, and the reaction is not initiated via 4,5-hydrogenation (see the Supporting Information for details).

Based on previous literature reports[28] and mechanistic experiments, a plausible hydrogenation mechanism is depicted in Scheme 7. The reaction begins with the coordination of $Mn(CO)_5Br$ with the chiral ligand to form complex **Mn−I**. Subsequently, in the presence of KO^{i}Pr, HBr is eliminated to yield complex **Mn−II**. Activation of hydrogen gas in the presence of KO^{i}Pr generates active species **I**, which then coordinates with substrate **1a** and promotes a synergistic transfer of a hydride, yielding intermediate **II**. Intermediate **II** undergoes a rapid proton-transfer reaction with HO^{i}Pr, forming *semi*-hydrogenated intermediate **Int-1** along with the generation of complex **III**. Isomerization of **Int-1** gives rise to two additional intermediates, **Int-2** and **Int-3**. Complex **III** is reactivated by hydrogen to regenerate active species **I**, which then coordinates with **Int-2**. This coordination enables another cycle of synergistic hydride transfer and proton transfer, ultimately producing target compound **2a**.

CONCLUSIONS

In summary, we successfully developed a series of chiral 2-hydroxypyridine-oxazoline bidentate phosphine-free ligands. These ligands demonstrated high efficacy in the manganese-catalyzed asymmetric hydrogenation of heteroaromatic pyrazolo[1,5-*a*]pyrimidines, simple ketones, and cyclic ketimines, achieving high yields and enantioselectivities. The mechanistic studies and DFT calculations supported that the motif 2-hydroxypyridine plays an important role in the synergistic metal activation of the hydrogen and hydride transfer pathway, highlighting the suitability of these ligands for asymmetric catalysis. This work not only underscores the potential of the chiral 2-hydroxypyridine-oxazoline ligands in asymmetric hydrogenation but also sets the stage for their application in a broader range of other catalytic reactions.

https://doi.org/10.1021/acscatal.4c06422
ACS Catal. 2025, 15, 3418−3427

Scheme 7. Plausible Mn-Catalyzed Hydrogenation Mechanism

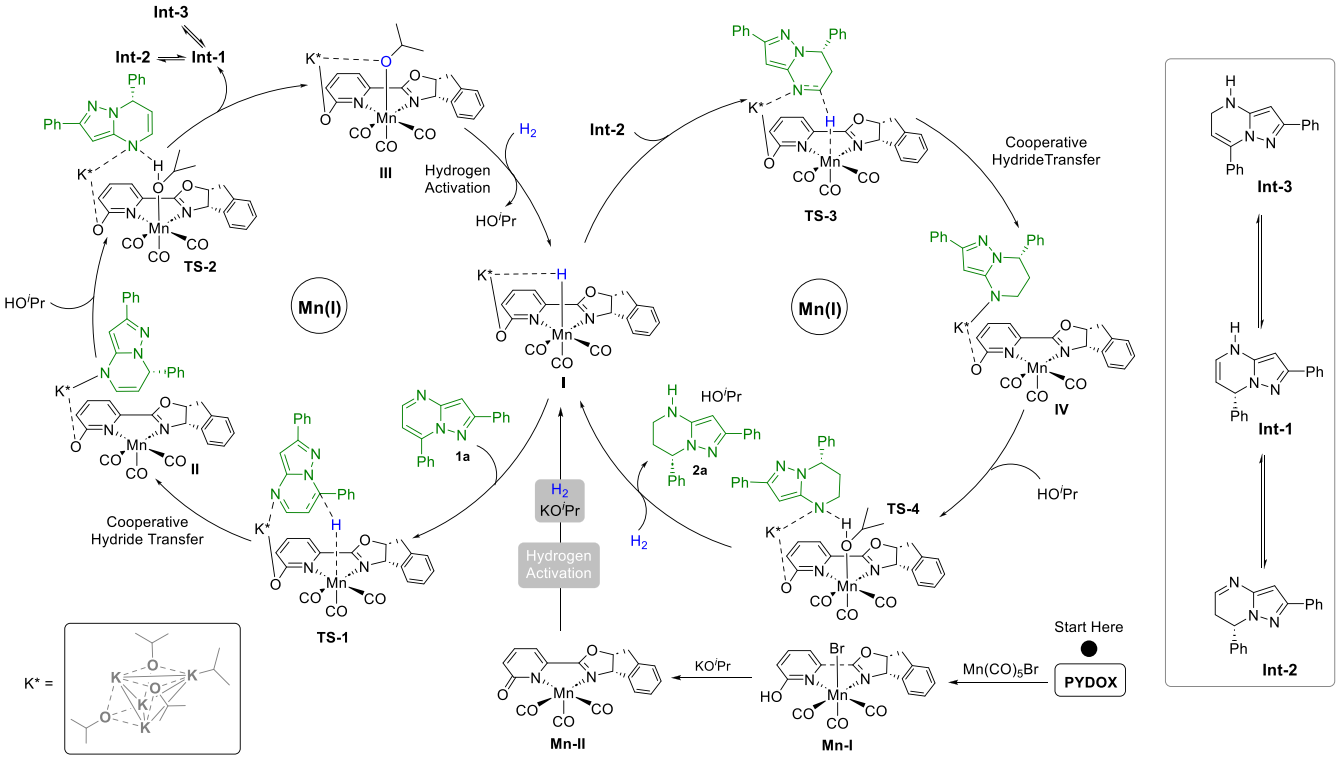

Ongoing research in our laboratory aims to expand the utility of these ligands and further elucidate their mechanistic properties.

■ ASSOCIATED CONTENT

Supporting Information

The Supporting Information is available free of charge at https://pubs.acs.org/doi/10.1021/acscatal.4c06422.

Detailed experimental procedures, characterization of new compounds, spectra, and X-ray data (PDF)

X-ray structure of ligand PYDOX L1 (CIF)

X-ray structure of complex $Mn(CO)_3$L6Br (CIF)

■ AUTHOR INFORMATION

Corresponding Authors

Mu-Wang Chen − *State Key Laboratory of Catalysis, Dalian Institute of Chemical Physics, Chinese Academy of Sciences, Dalian 116023, P. R. China;* orcid.org/0000-0001-6493-1363; Email: chemmuwang@dicp.ac.cn

Rong-Zhen Liao − *School of Chemistry and Chemical Engineering, Huazhong University of Science and Technology, Wuhan 430074, P. R. China;* orcid.org/0000-0002-8989-6928; Email: rongzhen@hust.edu.cn

Yong-Gui Zhou − *State Key Laboratory of Catalysis, Dalian Institute of Chemical Physics, Chinese Academy of Sciences, Dalian 116023, P. R. China;* orcid.org/0000-0002-3321-5521; Email: ygzhou@dicp.ac.cn

Authors

Gao-Wei Wang − *School of Chemistry, Dalian University of Technology, Dalian 116024, P. R. China*

Ya-Qi Wu − *School of Chemistry and Chemical Engineering, Huazhong University of Science and Technology, Wuhan 430074, P. R. China*

Qing-Xian Xie − *State Key Laboratory of Catalysis, Dalian Institute of Chemical Physics, Chinese Academy of Sciences, Dalian 116023, P. R. China*

Zheng Liu − *State Key Laboratory of Catalysis, Dalian Institute of Chemical Physics, Chinese Academy of Sciences, Dalian 116023, P. R. China*

Complete contact information is available at: https://pubs.acs.org/10.1021/acscatal.4c06422

Notes

The authors declare no competing financial interest.

■ ACKNOWLEDGMENTS

Financial support from the National Key Research and Development Program of China (2023YFA1507500), the National Natural Science Foundation of China (22371276), and the Dalian Institute of Chemical Physics (DICP I202404 and I202241) is acknowledged.

■ REFERENCES

(1) For selected reviews: (a) Filonenko, G. A.; van Putten, R.; Hensen, E. J. M.; Pidko, E. A. Catalytic (De)Hydrogenation Promoted by Non-precious Metals − Co, Fe and Mn: Recent Advances in an Emerging Field. *Chem. Soc. Rev.* **2018**, *47*, 1459−1483. (b) Alig, L.; Fritz, M.; Schneider, S. First-Row Transition Metal (De)Hydrogenation Catalysis Based on Functional Pincer Ligands. *Chem. Rev.* **2019**, *119*, 2681−2751. (c) Das, K.; Waiba, S.; Jana, A.; Maji, B. Manganese-Catalyzed Hydrogenation, Dehydrogenation, and Hydroelementation Reactions. *Chem. Soc. Rev.* **2022**, *51*, 4386−4464. (d) Wang, Y.; Wang, M.; Li, Y.; Liu, Q. Homogeneous Manganese-Catalyzed Hydrogenation and Dehydrogenation Reactions. *Chem.* **2021**, *7*, 1180−1223.

(2) (a) Elangovan, S.; Topf, C.; Fischer, S.; Jiao, H.; Spannenberg, A.; Baumann, W.; Ludwig, R.; Junge, K.; Beller, M. Selective Catalytic Hydrogenations of Nitriles, Ketones, and Aldehydes by Well-Defined

Manganese Pincer Complexes. *J. Am. Chem. Soc.* **2016**, *138*, 8809−8814. (b) Garbe, M.; Junge, K.; Walker, S.; Wei, Z.; Jiao, H.; Spannenberg, A.; Bachmann, S.; Scalone, M.; Beller, M. Manganese-(I)-Catalyzed Enantioselective Hydrogenation of Ketones Using a Defined Chiral PNP Pincer Ligand. *Angew. Chem., Int. Ed.* **2017**, *56*, 11237−11241.

(3) For selected NNP ligands examples: (a) Widegren, M. B.; Harkness, G. J.; Slawin, A. M.; Cordes, D. B.; Clarke, M. L. A highly Active Manganese Catalyst for Enantioselective Ketone and Ester Hydrogenation. *Angew. Chem., Int. Ed.* **2017**, *56*, 5825−5828. (b) Liu, C.; Wang, M.; Liu, S.; Wang, Y.; Peng, Y.; Lan, Y.; Liu, Q. Manganese-Catalyzed Asymmetric Hydrogenation of Quinolines Enabled by $\pi-\pi$ Interaction. *Angew. Chem., Int. Ed.* **2021**, *60*, 5108−5113. (c) Ling, F.; Hou, H.; Chen, J.; Nian, S.; Yi, X.; Wang, Z.; Song, D.; Zhong, W. Highly Enantioselective Synthesis of Chiral Benzhydrols *via*Manganese Catalyzed Asymmetric Hydrogenation of Unsymmetrical Benzophenones Using an Imidazole-Based Chiral PNN Tridentate Ligand. *Org. Lett.* **2019**, *21*, 3937−3941. (d) Zhang, L.; Wang, Z.; Han, Z.; Ding, K. Manganese-Catalyzed *anti*-Selective Asymmetric Hydrogenation of α-Substituted β-Ketoamides. *Angew. Chem., Int. Ed.* **2020**, *59*, 15565−15569.

(4) For selected PNP ligands examples: (a) Garbe, M.; Junge, K.; Walker, S.; Wei, Z.; Jiao, H.; Spannenberg, A.; Bachmann, S.; Scalone, M.; Beller, M. Manganese(I)-Catalyzed Enantioselective Hydrogenation of Ketones Using a Defined Chiral PNP Pincer Ligand. *Angew. Chem., Int. Ed.* **2017**, *56*, 11237−11241. (b) Zeng, L.; Yang, H.; Zhao, M.; Wen, J.; Tucker, J. H. R.; Zhang, X. C1-Symmetric PNP Ligands for Manganese-Catalyzed Enantioselective Hydrogenation of Ketones: Reaction Scope and Enantioinduction Model. *ACS Catal.* **2020**, *10*, 13794−13799. (c) Seo, C. S. G.; Tsui, B. T. H.; Gradiski, M. V.; Smith, S. A. M.; Morris, R. H. Enantioselective Direct, Base-Free Hydrogenation of Ketones by a Manganese Amido Complex of a Homochiral, Unsymmetrical P−N−P′ ligand. *Catal. Sci. Technol.* **2021**, *11*, 3153−3163.

(5) Bruneau-Voisine, A.; Wang, D.; Dorcet, V.; Roisnel, T.; Darcel, C.; Sortais, J.-B. Transfer Hydrogenation of Carbonyl Derivatives Catalyzed by an Inexpensive Phosphine-Free Manganese Precatalyst. *Org. Lett.* **2017**, *19*, 3656−3659.

(6) For selected examples: (a) van Putten, R.; Filonenko, G. A.; Gonzalez de Castro, A.; Liu, C.; Weber, M.; Muller, C.; Lefort, L.; Pidko, E. Mechanistic Complexity of Asymmetric Transfer Hydrogenation with Simple Mn-Diamine Catalysts. *Organometallics* **2019**, *38*, 3187−3196. (b) Wang, L.; Lin, J.; Sun, Q.; Xia, C.; Sun, W. Amino Acid Derived Chiral Aminobenzimidazole Manganese Catalysts for Asymmetric Transfer Hydrogenation of Ketones. *ACS Catal.* **2021**, *11*, 8033−8041.

(7) Shima, S.; Pilak, O.; Vogt, S.; Schick, M.; Stagni, M. S.; Meyer-Klaucke, W.; Warkentin, E.; Thauer, R. K.; Ermler, U. The Crystal Structure of [Fe]-Hydrogenase Reveals the Geometry of the Active Site. *Science* **2008**, *321*, 572−575.

(8) (a) Drover, M. W.; Love, J. A.; Schafer, L. L. 1,3-*N*,*O*-Complexes of Late Transition Metals. Ligands with Flexible Bonding Modes and Reaction Profiles. *Chem. Soc. Rev.* **2017**, *46*, 2913−2940. (b) Fedulin, A.; Jacobi von Wangelin, A. 2-Pyridonates: A Versatile Ligand Platform in 3d Transition Metal Coordination Chemistry and Catalysis. *Catal. Sci. Technol.* **2024**, *14*, 26−42.

(9) For selected examples for hydrogenation: (a) Yamaguchi, R.; Ikeda, C.; Takahashi, Y.; Fujita, K.-I. Homogeneous Catalytic System for Reversible Dehydrogenation-Hydrogenation Reactions of Nitrogen Heterocycles with Reversible Interconversion of Catalytic Species. *J. Am. Chem. Soc.* **2009**, *131*, 8410−8412. (b) Dubey, A.; Nencini, L.; Fayzullin, R. R.; Nervi, C.; Khusnutdinova, J. R. Bio-Inspired Mn(I) Complexes for the Hydrogenation of CO_2 to Formate and Formamide. *ACS Catal.* **2017**, *7*, 3864−3868.

(10) For selected examples transfer hydrogenation: (a) Moore, C. M.; Szymczak, N. K. 6,6-Dihydroxy Terpyridine: A Proton-Responsive Bifunctional Ligand and Its Application in Cataytic Transfer Hydrogenation of Ketones. *Chem. Commun.* **2013**, *49*, 400−402. (b) Wang, R.; Han, X.; Xu, J.; Liu, P.; Li, F. Transfer Hydrogenation of Ketones and Imines with Methanol under Base-Free Conditions Catalyzed by an Anionic Metal-Ligand Bifunctional Iridium Catalyst. *J. Org. Chem.* **2020**, *85*, 2242−2249.

(11) For selected examples for dehydrogenation: (a) Fujita, K.-I.; Tanino, N.; Yamaguchi, R. Ligand-Promoted Dehydrogenation of Alcohols Catalyzed by Cp*Ir Complexes. a New Catalytic System for Oxidant-Free Oxidation of Alcohols. *Org. Lett.* **2007**, *9*, 109−111. (b) Fujita, K. i.; Tamura, R.; Tanaka, Y.; Yoshida, M.; Onoda, M.; Yamaguchi, R. Dehydrogenative Oxidation of Alcohols in Aqueous Media Catalyzed by a Water-Soluble Dicationic Iridium Complex Bearing a Functional *N*-heterocyclic Carbene Ligand without Using Base. *ACS Catal.* **2017**, *7*, 7226−7230.

(12) For selected examples for dehydrogenation tandem reactions: (a) Li, F.; Ma, J.; Wang, N. α-Alkylation of Ketones with Primary Alcohols Catalyzed by a Cp*Ir Complex Bearing a Functional Bipyridonate Ligand. *J. Org. Chem.* **2014**, *79*, 10447−10455. (b) Fan, H.; Zhang, W.; Zhao, W.; Li, F. Acceptorless Dehydrogenative Cyclization of *o*-Aminobenzyl Amines and Aldehydes to Quinazolines in Water Catalyzed by a Water-Soluble Metal-Ligand Bifunctional Catalyst. *ChemistrySelect* **2017**, *2*, 5735−5739.

(13) For selected examples C-H activation: (a) Wang, P.; Li, G.-H.; Jain, P.; Farmer, M. E.; He, J.; Shen, P.-X.; Yu, J.-Q. Ligand-Promoted meta-C-H Amination and Alkynylation. *J. Am. Chem. Soc.* **2016**, *138*, 14092−14099. (b) Li, G.; Wang, P.; Farmer, M. E.; Farmer, M. E.; Yu, J.-Q. Ligand-Enabled Auxiliary-Free *meta*-C-H Arylation of Phenylacetic Acids. *Angew. Chem., Int. Ed.* **2017**, *56*, 6874−6877. (c) Wang, P.; Verma, P.; Xia, G.; Shi, J.; Qiao, J. F.; Tao, S.; Cheng, P. W.; Poss, M. A.; Farmer, M. E.; Yeung, K.-S.; Yu, J.-Q. Ligand-Accelerated Non-Directed C−H Functionalization of Arenes. *Nature* **2017**, *551*, 489−494. (d) Li, Z.; Wang, Z.; Chekshin, N.; Qian, S.; Qiao, J. X.; Cheng, P. T.; Yeung, K. S.; Ewing, W. R.; Yu, J.-Q. A Tautomeric Ligand Enables Directed C−H Hydroxylation with Molecular Oxygen. *Science* **2021**, *372*, 1452−1457.

(14) Yuan, C.-H.; Wang, X.-X.; Jiao, L. Ligand-Enabled Palladium-(II)-Catalyzed Enantioselective β-C(sp^3)−H Arylation of Aliphatic Tertiary Amides. *Angew. Chem., Int. Ed.* **2023**, *62*, No. e202300854.

(15) For selected reviews: (a) Yang, G.; Zhang, W. Renaissance of Pyridine-Oxazolines as Chiral Ligands for Asymmetric Catalysis. *Chem. Soc. Rev.* **2018**, *47*, 1783−1810. (b) Connon, R.; Roche, B.; Rokade, B. V.; Guiry, P. J. Further Developments and Applications of Oxazoline-Containing Ligands in Asymmetric Catalysis. *Chem. Rev.* **2021**, *121*, 6373−6521.

(16) Shimbayashi, T.; Fujita, K.-I. Recent Advances in Homogeneous Catalysis *via* Metal−Ligand Cooperation Involving Aromatization and Dearomatization. *Catalysis* **2020**, *10*, 635.

(17) (a) Zhou, Y.-G.; Wang, G.-W.; Chen, M.-W.; Sun, L. Preparation Method and Application of Chiral Hydroxypyridine Oxazoline Skeleton Compound and Derivative Thereof. 10368894.9 A, 2023. (b) Very recently, Yu's group reported a similar route for synthesis of three chiral hydroxypyridine-oxazoline ligands and application in asymmetric C−H activation, but they exhibited low activity and selectivity. see Zhang, T.; Zhang, Z.-Y.; Kang, G.; Sheng, T.; Yan, J. L.; Yang, Y. B.; Ouyang, Y.; Yu, J.-Q. Enantioselective Remote Methylene C-H (hetero)Arylation of Cycloalkane Carboxylic Acids. *Science* **2024**, *384*, 793−798.

(18) Xi, T.; Mei, Y.; Lu, Z. Palladium-Catalyzed C-2 C-H Heteroarylation of Chiral Oxazolines: Diverse Synthesis of Chiral Oxazoline Ligands. *Org. Lett.* **2015**, *17*, 5939−5941.

(19) Deng, D.; Hu, B.; Zhang, Z.; Mo, S.; Yang, M.; Chen, D.-F. Alkylation of Aromatic Amines with Trialkyl Amines Catalyzed by a Defined Iridium Complex with a 2-Hydroxypyridyl- methylene Fragment. *Organometallics* **2019**, *38*, 2218−2226.

(20) Garduño, J. A.; García, J. J. Synthesis of Amidines and Benzoxazoles from Activated Nitriles with Ni(0) Catalysts. *ACS Catal.* **2015**, *5*, 3470−3477.

(21) For selected examples: (a) Guo, Y.; Liu, Y.; Hu, N.; Yu, D.; Zhou, C.; Shi, G.; Zhang, B.; Wei, M.; Liu, J.; Luo, L.; Tang, Z.; Song, H.; Guo, Y.; Liu, X.; Su, D.; Zhang, S.; Song, X.; Zhou, X.; Hong, Y.; Chen, S.; Cheng, Z.; Young, S.; Wei, Q.; Wang, H.; Wang, Q.; Lv, L.;

https://doi.org/10.1021/acscatal.4c06422
ACS Catal. 2025, 15, 3418−3427

Wang, F.; Xu, H.; Sun, H.; Xing, H.; Li, N.; Zhang, W.; Wang, Z.; Liu, G.; Sun, Z.; Zhou, D.; Li, W.; Liu, L.; Wang, L.; Wang, Z. Discovery of Zanubrutinib (BGB-3111), a Novel, Potent, and Selective Covalent Inhibitor of Bruton's Tyrosine Kinase. *J. Med. Chem.* **2019**, *62*, 7923−7940. (b) Barlaam, B.; Casella, R.; Cidado, J.; Cook, C.; De Savi, C.; Dishington, A.; Donald, C. S.; Drew, L.; Ferguson, A. D.; Ferguson, D.; Glossop, S.; Grebe, T.; Gu, C.; Hande, S.; Hawkins, J.; Hird, A. W.; Holmes, J.; Horstick, J.; Jiang, Y.; Lamb, M. L.; McGuire, T. M.; Moore, J.; O'Connell, E. N.; Pike, A.; Pike, K. G.; Proia, T.; Roberts, B.; San Martin, M.; Sarkar, U.; Shao, W.; Stead, D.; Sumner, N.; Thakur, K.; Vasbinder, M. M.; Varnes, J. G.; Wang, J.; Wang, L.; Wu, D.; Wu, L.; Yang, B.; Yao, T. Discovery of AZD4573, a Potent and Selective Inhibitor of CDK9 That Enables Short Duration of Target Engagement for the Treatment of Hematological Malignancies. *J. Med. Chem.* **2020**, *63*, 15564−15590.

(22) (a) Alvarez-Ruzi, E.; Ballell-Pages, L.; Castro-Pichel, J.; Encinas, L.; Esquivias, J.; Gamo-Benito, F. J.; Garcia-Palancar, M. C.; Remuinan-Blance, M. J. Composés Antituberculeux à Base de Tétrahydropyrazolo[1,5-a]pyrimidine, WO 2012143522 A1, 2012. (b) Wang, L.; Song, J.; Zhang, T.; Li, K.; Luo, L.; Wei, M.; Wang, Z.; Guo, Y. WO Patent, WO033135 A12018.

(23) (a) Glorius, F. Asymmetric Hydrogenation of Aromatic Compounds. *Org. Biomol. Chem.* **2005**, *3*, 4171−4175. (b) Wang, D.-S.; Chen, Q.-A.; Lu, S.-M.; Zhou, Y.-G. Asymmetric Hydrogenation of Heteroarenes and Arenes. *Chem. Rev.* **2012**, *112*, 2557−2590. (c) Kim, A. N.; Stoltz, B. M. Recent Advances in Homogeneous Catalysts for the Asymmetric Hydrogenation of Heteroarenes. *ACS Catal.* **2020**, *10*, 13834−13851.

(24) (a) Xie, C.; Xiao, G.; Guo, Q.; Wu, X.; Zi, G.; Ding, W.; Hou, G. Highly Enantioselective Rh-catalyzed Asymmetric Reductive Dearomatization of Multi-nitrogen Polycyclic Pyrazolo[1,5-*a*]-pyrimidines. *Chem. Sci.* **2023**, *14*, 9048−9054. (b) Yuan, H.; Yao, W.; Zhang, X.; Wei, Z.; Xi, J.; Hao, Y.; Liu, X.; Jiang, R.; Nie, H. Highly Enantioselective Ir-Catalyzed Hydrogenation of Pyrazolo[1,5-*a*]pyrimidine for the Synthesis of Zanubrutinib. *J. Org. Chem.* **2024**, *89*, 1748−1752. (c) Li, B.; Zhou, G.; Zhang, D.; Yao, L.; Li, M.; Yang, G.; Zhang, S.; Nie, H. Spiro-Josiphos Ligands for the Ir-Catalyzed Asymmetric Synthesis of Chiral Amines under Hydrogenation Conditions. *Org. Lett.* **2024**, *26*, 2097−2102. (d) Chen, M.-W.; Li, H.-W.; Wang, Y.-Q.; Wu, B.; Liu, Z.; Lai, X.; Deerberg, J.; Zhou, Y.-G. Iridium-Catalyzed Asymmetric Hydrogenation of Heteroaromatics with Multiple *N* Atoms *via* Substrate Activation: An Entry to 4,5,6,7-Tetrahydropyrazolo[1,5-*a*]pyrimidine-3-carbonitrile Core of a Potent BTK Inhibitor. *J. Org. Chem.* **2024**, *89*, 4336−4348.

(25) (a) Maji, M.; Kundu, S. Cooperative Ruthenium Complex Catalyzed Multicomponent Synthesis of Pyrimidines. *Dalton Trans.* **2019**, *48*, 17479−17487. (b) Nandi, S.; Borthakur, I.; Ganguli, K.; Kundu, S. 2-(2-Benzimidazolyl)pyridine Mn(I) Complexes: Synthesis and Exploration of Catalytic Activity toward Synthesis of Pyrimidine and Quinoline. *Organometallics* **2023**, *42*, 1793−1802.

(26) CCDC 2328157 contains supplementary crystallographic data of Mn(PYDOX L6)$(CO)_3$Br.

(27) (a) Ohkuma, T.; Ooka, H.; Hashiguchi, S.; Ikariya, T.; Noyori, R. Practical Enantioselective Hydrogenation of Aromatic Ketones. *J. Am. Chem. Soc.* **1995**, *117*, 2675−2676. (b) Dub, P. A.; Henson, N. J.; Martin, R. L.; Gordon, J. C. Unravelling the Mechanism of the Asymmetric Hydrogenation of Acetophenone by [RuX 2-(diphosphine)(1,2-diamine)] Catalysts. *J. Am. Chem. Soc.* **2014**, *136*, 3505−3521. (c) Dub, P. A.; Gordon, J. C. The Role of Metal-Bound N-H Functionality in Noyori-Type Molecular Catalysts. *Nat. Rev. Chem* **2018**, *2*, 396−408.

(28) (a) Wang, Y.; Liu, S.; Yang, H.; Li, H.; Lan, Y.; Liu, Q. Structure Reactivity and Catalytic Properties of Manganese-Hydride Amidate Complexes. *Nat. Chem.* **2022**, *14*, 1233−1241. (b) Wang, Y.; Zhu, L.; Shao, Z.; Li, G.; Lan, Y.; Liu, Q. Unmasking the Ligand Effect in Manganese-Catalyzed Hydrogenation: Mechanistic Insight and Catalytic Application. *J. Am. Chem. Soc.* **2019**, *141*, 17337−17349. (c) Wang, M.; Liu, S.; Liu, H.; Wang, Y.; Lan, Y.; Liu, Q. Asymmetric hydrogenation of ketimines with minimally different alkyl groups. *Nature* **2024**, *631*, 556−562.

(29) For computational details, see Supporting Information.

(30) (a) Stanton, M. G.; Gagne, M. R. The Remarkable Catalytic Activity of Alkali-MetalAlkoxide Clusters in the Ester Interchange Reaction. *J. Am. Chem. Soc.* **1997**, *119*, 5075−5076. (b) Liu, W. B.; Schuman, D. P.; Yang, Y. F.; Toutov, A. A.; Liang, Y.; Klare, H. F. T.; Nesnas, N.; Oestreich, M.; Blackmond, D. G.; Virgil, S. C.; Banerjee, S.; Zare, R. N.; Grubbs, R. B.; Houk, K. N.; Stoltz, B. M. Potassium tert-Butoxide-Catalyzed Dehydrogenative C−H Silylationof Heteroaromatics: A Combined Experimental and Computational Mechanistic Study. *J. Am. Chem. Soc.* **2017**, *139*, 6867−6879.

(31) Falivene, L.; Cao, Z.; Petta, A.; Serra, L.; Poater, A.; Oliva, R.; Scarano, V.; Cavallo, L. Towards the Online Computer-Aided Design of Catalytic Pockets. *Nat. Chem.* **2019**, *11*, 872−879.

(32) (a) Lu, T.; Chen, F. Multiwfn: A Multifunctional Wavefunction Analyzer. *J. Comput. Chem.* **2012**, *33*, 580−592. (b) Lu, T.; Chen, Q. X. Simple, Efficient, and Universal Energy Decomposition Analysis Method Based on Dispersion-Corrected Density Functional Theory. *J. Phys. Chem. A* **2023**, *127*, 7023−7035.

https://doi.org/10.1021/acscatal.4c06422
ACS Catal. 2025, 15, 3418−3427